Electronic Supporting Information

Quantum Chemical Prediction of a Superelectrophilic Dianion and its Binding with Noble Gas atoms

Meenakshi Joshi[a,b] and Tapan K. Ghanty[a,b,*]

[a]Theoretical Chemistry Section, Chemistry Group, Bhabha Atomic Research Centre, Mumbai 400085, India.

[b]Homi Bhabha National Institute, Training School Complex, Anushakti Nagar, Mumbai–400094, India.

Computational Details

In the present work, all the calculations are performed using Turbomole 7.2 program.[1] The $[NgBeB_{11}(CN)_{11}]^{2-}$ and $[(Ng)_2BeB_{11}(CN)_{10}]^{-}$ systems are optimized using MP2[2] and dispersion−corrected[3] density functional theory (DFT−D3) with B3LYP and PBE0 functionals[4]. For all the atoms def−TZVPP basis set is used except for Xe for which def2−TZVPP basis set has been used along with 60 electron core ECP.[5] Frequency calculations has been performed with B3LYP-D3 and PBE0-D3 functionals along with def-TZVPP basis set to obtain minimum energy structure. The $[NgBeB_{11}(CN)_{11}]^{2-}$ and $[(Ng)_2BeB_{11}(CN)_{10}]^{-}$ systems are optimized with all real frequencies only. For benchmarking NgBeO compounds are optimized using CCSD(T)[6] method using aug−cc−pVTZ (AVTZ) basis set using MOLPRO2012[7] software, B3LYP−D3, PBE0−D3 and MP2 methods using Turbomole 7.2 program. Charge distribution analysis is performed using natural population analysis (NPA) scheme.[8] Furthermore, to get the clear insight into the nature of chemical bond we have performed the AIM (atoms–in–molecule) analysis[9] at B3LYP−D3/def−TZVPP level employed with energy density function (EDF)[10] for Xe atom using Multiwfn program[11]. For Ng-Dianion**1** compounds the binding energy is calculated using DLPNO-CCSD(T) method[12] with def2-TZVP basis set as implemented in ORCA3.0.3 program.[13] In addition free energy of Ng-Dianion1 compounds has been calculated at 298K temperature with B3LYP−D3BJ/def2−TZVP method using ORCA 3.0.3 program. Moreover, energy decomposition analysis in conjunction with the natural orbital for chemical valence (EDA-NOCV)[14] has been performed on the B3LYP−D3/def-TZVPP optimized geometry in ADF2017 software[15a,15b] using B3LYP−D3 functional and TZ2P[15c] basis set. For heavy atom scalar relativistic effect[16] has been included in the calculation. In EDA-NOCV, total deformation density ($\Delta\rho(r)$) is decomposed into its individual differential densities ($\Delta\rho_i(r)$), ($\Delta\rho(r) = \sum\Delta\rho_i(r)$) which can be represented in the pairs of NOCV. The NOCV pairs of deformation density give the direction of the charge flow in between those fragments. Similarly, the total ΔE^{orb} is decomposed into ΔE_i^{orb} ($\Delta Eorb = \sum\Delta E_i^{orb}$) corresponding to each charge transfer channel. For $[(Ng)_2BeB_{11}(CN)_{10}]^{-}$ and $\{Li^+[NgBeB_{11}(CN)_{11}]^{2-}\}$ compounds the binding energy (BE) has been calculation using following Equation S1 and S2, respectively.

$$BE = E[(Ng)_2BeB_{11}(CN)_{10}]^{-} - 2* E(Ng) - E[BeB_{11}(CN)_{10}]^{-} \qquad (S1)$$

$$BE = \{Li^+[NgBeB_{11}(CN)_{11}]^{2-}\} - E(Ng) - \{Li^+[BeB_{11}(CN)_{11}]^{2-}\} \qquad (S2)$$

References

1. TURBOMOLE is program package developed by the Quantum Chemistry Group at the University of Karlsruhe, Germany, 1988: Ahlrichs, R.; Bär, M.; Häser, M.; Horn, H.; Kölmel, C. *Chem. Phys. Lett.* **1989**, *162*, 165−169.
2. M. J. Frisch, M. Head−Gordon, J. A. Pople, *Chem. Phys. Lett.* **1990**, *166*, 275−280.
3. a) S. Grimme, J. Antony, S. Ehrlich, H. A Krieg, *J. Chem. Phys*. **2010**, *132*, 154104. b) S. Grimme, A. Hansen, J. G. Brandenburg, C. Bannwarth, *Chem. Rev.* **2016**, *116*, 5105−5154.
4. a) A. D. Becke, *J. Chem. Phys.* **1993**, *98*, 1372−1377. b) C. Lee, W. Yang, R. G. Parr, *Phys. Rev. B* **1988***, 37*, 785−789. c) A. D. Becke, *Phys. Rev. A* **1988**, *38*, 3098−3100. d) C. Adamo, V. Barone, *J. Chem. Phys.* **1999**, *110*, 6158.
5. a) F. Weigenda, R. Ahlrichs, *Phys. Chem. Chem. Phys.* **2005**, *7*, 3297–3305. b) A. Schäfer, C. Huber, R. Ahlrichs, *J. Chem. Phys.* **1994**, *100*, 5829. C) K. A. Peterson, D. Figgen, E. Goll, H. Stoll, M. Dolg, *J. Chem. Phys.* **2003**, *119*, 11113.
6. C. Hampel, K. Peterson, H.−J. Werner, *Chem. Phys. Lett.* **1992**, *190*, 1−12.
7. H.−J. Werner, P. J. Knowles, G. Knizia, F. R. Manby, M. Schützet, P. Celani, T. Korona, R. Lindh, A. Mitrushenkov, G. Rauhut, et al. MOLPRO, version 2012.1, a Package of ab initio Programs, **2012**; see http://www.molpro.net.
8. A. E. Reed, R. B. Weinstock, F. A. Weinhold, *J. Chem. Phys*. **1985**, *83*, 735−−npa
9. a) R. F. W. Bader, Atoms in Molecules−A Quantum Theory; *Oxford University Press: Oxford, U.K.,* **1990**. b) W. Zou, D. Nori−Shargh, Boggs, *J. Phys. Chem. A* **2013**, *117*, 207−212.
10. T. A. Keith, M. J. Frisch, *J. Phys. Chem. A*. **2011**, *115*, 12879–12894.
11. T. Lu, F. W. Chen, *J. Comput. Chem.* **2012**, *33*, 580−592.
12. (a) Riplinger, B. Sandhoefer, A. Hansen and F. Neese, J. Chem. Phys., 2013, 139, 134101. (b) C. Riplinger, P. Pinski, U. Becker, E. F. Valeev and F. Neese, J. Chem. Phys., 2016, 144, 024109. (c) D. G. Liakos, F. Neese, *J. Chem. Theory Comput.* **2015**, *11*, 4054–4063.
13. F. Neese, F. Wennmohs, U. Becker, D. Bykov, D. Ganyushin, A. Hansen, R. Izsaɳk, D. G. Liakos, C. Kollmar, S. Kossmann, D. A. Pantazis, ORCA, version 3.0.3; Max Planck Institute for Chemical Energy Conversion: Mülheim/Ruhr, Germany, 2014.

14. (a) T. Ziegler and A. Rauk, *Theor. Chim. Acta.,* 1977, **46**, 1−10. b) M. P. Mitoraj, A. Michalak, T. A. Ziegler, *J. Chem. Theory Comput.* **2009**, *5*, 962−975. c) M. P. Mitoraj, A. Michalak, *Organometallics* **2007**, *26*, 6576−6580.
15. a) ADF2017; SCM, Theoretical Chemistry, Vrije Universiteit: Amsterdam, The Netherlands. http://www.scm.com. b) G. te Velde, F. M. Bickelhaupt, S. A. van Gisbergen, C. Fonseca Guerra, E. J. Baerends, J. G. Snijders, T. Ziegler, *J. Comput. Chem.* **2001**, *22*, 931−967. c) E. van Lenthe, E. J. Baerends, *J. Comput. Chem.* **2003**, *24*, 1142–1156.
16. a) E. van Lenthe, E. J. Baerends, J. G. Snijders, *J. Chem. Phys.* **1994**, *101*, 9783–9792. b) E. van Lenthe, A. E. Ehlers, E. J. Baerends, *J. Chem. Phys.* **1999**, *110*, 8943–8953.

List of Tables

Table S7. Optimized Ng−B Bond Length (R(Ng−B), in Å), Binding Energy (BE, in kcal mol^{-1}), NPA charges on the B and Ng Atom (q_B and q_{Ng}, in e) of $[NgB_{12}(CN)_{11}]^{-}$ Compounds in C_{5v} Symmetry using B3LYP−D3/def−TZVPP and PBE0/def−TZVPP Methods and in C_5 symmetry using MP2 Method. PBE0−D3 Results are provided in the Parenthesis. ZPE Corrected Binding Energy are Reported with B3LYP−D3 and PBE0−D3 Methods.

Table S8. Optimized Ng−B Bond Length (R(Ng−B), in Å), Binding Energy (BE, in kcal mol^{-1}), NPA charges on the B and Ng Atom (q_B and q_{Ng}, in e) of $[NgB_{12}(Cl)_{11}]^{-}$ Compounds in C_{5v} Symmetry using B3LYP−D3/def−TZVPP and PBE0/def−TZVPP Methods and in C_5 symmetry using MP2 Method. PBE0−D3 Results are provided in the Parenthesis. ZPE Corrected Binding Energy are Reported with B3LYP−D3 and PBE0−D3 Methods.

Table S9. Optimized Ng−B Bond Length (R(Ng−Be), in Å), ZPE Corrected Binding Energy (BE, in kcal mol^{-1}), NPA charges on the Be, Li and Ng Atoms (q_B, q_{Li} and q_{Ng}, in e) of $\{Li^{+}@[NgBeB_{11}(CN)_{11}]^{2-}\}$ Compounds using B3LYP−D3/def−TZVPP and Method.

Table S10. ZPE Corrected Relative Energy (RE, in kcal mol$^{-1)}$ of Ng_2−Anion**3**[a] $[1,12-(Ng)_2BeB_{11}(CN)_{10}]^{-}$ with respect to Ng_2−Anion**2**[b] $[1,7-(Ng)_2BeB_{11}(CN)_{10}]^{-}$ at B3LYP−D3/def−TZVPP level of theory. PBE0−D3/def−TZVPP Calculated Values are Provided within Parenthesis. HOMO-LUMO Energy Gap (ΔE_{gap}, in eV) using B3LYP-D3/def-TZVPP (PBE0-D3/def-TZVPP) Level of Theory is also Reported.

Table S11. Optimized Ng−B, Ng−Be Bond Length (R(Ng−B) and R(Ng−Be), in Å), ZPE Corrected Binding Energy (BE, in kcal mol^{-1}), NPA charges on the B, Be and Ng Atoms (q_B, q_{Be} and q_{Ng}, in e) of $[1,7\text{-}(Ng)_2BeB_{11}(CN)_{10}]^{-}$[a] Compounds using B3LYP−D3/def−TZVPP and PBE0−D3/def−TZVPP Methods.

Table S12. Optimized Ng−B, Ng−Be Bond Length (R(Ng−B) and R(Ng−Be), in Å), Binding Energy (BE, in kcal mol^{-1}), NPA charges on the B, Be and Ng Atoms (q_B, q_{Be} and q_{Ng}, in e) of $[1,12\text{-}(Ng)_2BeB_{11}(CN)_{10}]^{-}$[a] Compounds in C_{5v} Symmetry using B3LYP−D3/def−TZVPP, PBE0−D3/def−TZVPP Methods and in C_5 symmetry using MP2 Method. ZPE Corrected Binding Energy are Reported with B3LYP−D3 and PBE0−D3 Methods.

Table S13. Calculated Values of Bond Critical Point Electron Density (ρ in e a_0^{-3}), Laplacian of Electron Density ($\nabla^2\rho$ in e a_0^{-5}), Local Electron Energy Density (E_d in au), and Ratio of Local Electron Kinetic Energy Density and Electron Density ($G(\mathbf{r})/\rho$ in au) of Ng–B and Ng–Be bond in Ng–Dianion**1**, Ng–Dianion**2**, $[NgB_{12}(CN)_{11}]^-$, $[NgB_{12}(Cl)_{11}]^-$ and $[1,12\text{-}(Ng)_2BeB_{11}(CN)_{10}]^-$ (Ng_2-Anion**3)** using ^{a}B3LYP–D3/def–TZVPP method.

Table S14. The Calculated Values of Electrostatic Energy (ΔE^{elec}), Pauli Repulsion Energy (ΔE^{Pauli}), Orbital Interactions Energy (ΔE^{orb}), Dispersion Energy (ΔE^{disp}) and Total Interaction Energy (ΔE^{int}) of Ng–Dianion**2**^{a} Compounds in kcal mol^{-1} as obtained from Energy Decomposition Analysis at B3LYP–D3/def–TZVPP level of theory. (Percentage Contribution of ΔE^{elec}, ΔE^{orb} and ΔE^{disp} Energy term to the Total Interaction Energy are Provided within Parenthesis)

Table S15. The Calculated Values of Electrostatic Energy (ΔE^{elec}), Pauli Repulsion Energy (ΔE^{Pauli}), Orbital Interactions Energy (ΔE^{orb}), Dispersion Energy (ΔE^{disp}) and Total Interaction Energy (ΔE^{int}) of $[1,7\text{-}(Ng)_2BeB_{11}(CN)_{10}]^{-a}$ (Ng_2–Anion2) Compounds in kcal mol^{-1} as obtained from Energy Decomposition Analysis at B3LYP–D3/def–TZVPP level of theory. (Percentage Contribution of ΔE^{elec}, ΔE^{orb} and ΔE^{disp} Energy term to the Total Interaction Energy are Provided within Parenthesis)

List of Figures

Figure S1. Optimized Structures of Dianion**1** (with free Be1 atom), Dianion**2** (with free B2 atom), Dianion**3** (with free B7 atom) and Dianion**4** (with free B12 atom) of $[BeB_{11}(CN)_{11}]^{2-}$ at B3LYP-D3/def-TZVPP level of theory. Relative energy (RE, in kcal mol^{-1}) calculated using B3LYP-D3/def-TZVPP (PBE0-D3/def-TZVPP) is also reported.

Figure S2. ESP of Dianion**1** (on left) and Dianion**4** (on right) of $[BeB_{11}(CN)_{11}]^{2-}$. Red region is a electron–rich nucleophilic site and blue region is electron–deficient electrophilic site

Figure S3. Pictures of lowest unoccupied molecular orbital (LUMO) of different Isomers of Dianion $[BeB_{11}(CN)_{11}]^{2-}$ at B3LYP-D3/def-TZVPP level of theory.

Figure S4. Optimized structures of {$Li^+[XeBeB_{11}(CN)_{11}]^{2-}$} at B3LYP-D3/def-TZVPP level of theory.

Figure S5. Optimized Structures of Anion**1** [1,2-$BeB_{11}(CN)_{10}]^-$, Anion**2** [1,7-$BeB_{11}(CN)_{10}]^-$, Anion**3** [1,12-$BeB_{11}(CN)_{10}]^-$, and Anion**4** [5,6-$BeB_{11}(CN)_{10}]^-$, Anion**5** [5,10-$BeB_{11}(CN)_{10}]^-$ at B3LYP-D3/def-TZVPP level of theory. Relative energy (RE, in kcal mol^{-1}) calculated using B3LYP-D3/def-TZVPP (PBE0-D3/def-TZVPP) is also reported.

Figure S6. Pictures of lowest unoccupied molecular orbital (LUMO) of different Isomers of Anion $[BeB_{11}(CN)_{10}]^-$ at B3LYP-D3/def-TZVPP level of theory.

Figure S7. Deformation densities ($\Delta\rho$(r)) plots of the pairwise orbital interactions for Ng−Dianion**1** (Ng =He−Xe) complexes and the associated ΔE^{orb} energies (ΔE^{σ} and ΔE^{π} , in kcal mol^{-1}) obtained from the EDA−NOCV at B3LYP-D3/TZ2P level of theory. The blue and red colored surfaces indicate regions with $\Delta\rho(r) > 0$ and $\Delta\rho(r) < 0$, respectively.

Figure S8. Deformation densities ($\Delta\rho$(r)) plots of the pairwise orbital interactions for Ng−Dianion**2** (Ng =He−Xe) complexes and the associated ΔE^{orb} energies (ΔE^{σ} and ΔE^{π} , in kcal mol^{-1}) obtained from the EDA−NOCV at B3LYP-D3/TZ2P level of theory. The blue and red colored surfaces indicate regions with $\Delta\rho(r) > 0$ and $\Delta\rho(r) < 0$, respectively.

Figure S9. Deformation densities ($\Delta\rho$(r)) plots of the pairwise orbital interactions for Ng_2−Anion**2** (Ng =He−Xe) complexes and the associated ΔE^{orb} energies (ΔE^{σ} and ΔE^{π} , in kcal mol^{-1}) obtained from the EDA−NOCV at B3LYP-D3/TZ2P level of theory. The blue and red colored surfaces indicate regions with $\Delta\rho(r) > 0$ and $\Delta\rho(r) < 0$, respectively.

Table S1. Optimized Ng−Be Bond Length (in, Å) and Binding Energy (kcal mol^{-1}) of NgBeO Compounds Calculated using CCSD(T), MP2, B3LYP−D3 and PBE0−D3 Methods. ZPE Corrected Binding Energy are Reported with B3LYP−D3 and PBE0−D3 Methods. Binding Energy is Provided in the Parenthesis.

NgBeO	CCSD(T)[a]	MP2[b]	B3LYP−D3[b]	PBE0−D3[b]
HeBeO	1.524 (−5.0)	1.523 (−4.7)	1.492 (−5.4)	1.500 (−5.5)
NeBeO	1.796 (−5.2)	1.852 (−3.8)	1.794 (−5.0)	1.793 (−5.3)
ArBeO	2.075 (−11.9)	2.101 (−10.0)	2.069 (−11.4)	2.056 (−12.3)
KrBeO	2.210 (−14.0)	2.241 (−12.1)	2.211 (−13.4)	2.194 (−14.9)
XeBeO	2.385 (−17.0)	2.417 (−14.2)	2.391 (−15.7)	2.366 (−17.6)

[a] optimized using AVTZ basis set for all atoms along with ECP10MDF for Kr and ECP28MDF for Xe atoms using software Molpro2012.

[b] optimized using def−TZVPP basis set for all atoms except Xe for which def2−TZVPP basis set is used along with 28 electron core ECP using software Turbomole−7.2.

Binding energy as well as Ng−Be bond distance calculated using B3LYP−D3 method matches quite well with CCSD(T) values.

Table S2. First, Second and Third Electron Binding Affinity (EA1, EA2 and EA3, in kcal mol^{-1}) of Isomer1[a], Isomer2[b], Isomer3[c] and Isomer4[d] of Neutral $BeB_{11}(CN)_{11}$ compound at B3LYP-D3/def-TZVPP level of theory. HOMO-LUMO Energy Gap (ΔE_{gap}, in eV) Calculated using B3LYP-D3/def-TZVPP (PBE0-D3/def-TZVPP) Level of Theory is also Reported.

$BeB_{11}(CN)_{11}$	EA1	EA2	EA3	ΔE_{gap}
Isomer1	181.1	101.3	-54.4	4.78 (5.24)
Isomer2	185.4	100.0	-24.4	3.54 (3.91)
Isomer3	177.5	98.2	-15.5	3.06 (3.41)
Isomer4	177.8	96.3	-10.1	2.80 (3.15)

[a] Be1 atom has free binding site
[b] B2 atom has free binding site
[c] B7 atom has free binding site
[d] B12 atom has free binding site

where, $EA1 = E[BeB_{11}(CN)_{11}] - E[BeB_{11}(CN)_{11}]^{-}$ (1)

$EA2 = E[BeB_{11}(CN)_{11}]^{-} - E[BeB_{11}(CN)_{11}]^{2-}$ (2)

$EA3 = E[BeB_{11}(CN)_{11}]^{2-} - E[BeB_{11}(CN)_{11}]^{3-}$ (3)

Large value of second electron binding affinity as well as HOMO-LUMO energy gap represents high gas phase stability of the formed dianions.

Table S3. ZPE Corrected Relative Energy (RE, in kcal mol^{-1}) of Ng−B Compounds of Dianion2, Dianion3, Dianion4 with respect to the Ng−Be Compounds of Dianion1 at B3LYP−D3/def−TZVPP Level of Theory. PBE0-D3/def−TZVPP Calculated Values are Provided within Parenthesis. HOMO-LUMO Energy Gap (ΔE_{gap}, in eV) Calculated using B3LYP-D3/def-TZVPP (PBE0-D3/def-TZVPP) Level of Theory is also Reported.

Ng−Dianion		**Ng−Be**	**Ng−B**		
		Ng−Dianion1[a]	**Ng−Dianion2**[b]	**Ng−Dianion3**[c]	**Ng−Dianion4**[d]
He-Dianion	**RE**	0.0 (0.0)	28.1 (32.4)	36.1 (40.4)	41.5 (46.7)
	ΔE_{gap}	6.26 (6.63)	3.68 (4.03)	3.19 (3.54)	3.09 (4.32)
Ne−Dianion	**RE**	0.0 (0.0)	27.5 (32.1)	35.6 (40.1)	40.8 (45.4)
	ΔE_{gap}	5.89 (6.36)	3.71 (4.11)	3.29 (3.70)	3.12 (3.57)
Ar−Dianion	**RE**	0.0 (0.0)	29.3 (32.7)	35.8 (38.6)	39.6 (42.4)
	ΔE_{gap}	6.22 (6.58)	4.46 (5.17)	4.30 (4.97)	4.23 (4.90)
Kr−Dianion	**RE**	0.0 (0.0)	30.0 (30.8)	34.0 (36.4)	37.5 (39.8)
	ΔE_{gap}	6.21 (6.57)	4.60 (5.21)	4.36 (4.96)	4.24 (4.86)
Xe−Dianion	**RE**	0.0 (0.0)	26.0 (28.1)	31.5 (31.8)	34.7 (36.5)
	ΔE_{gap}	6.19 (6.57)	4.52 (5.09)	4.21 (4.97)	4.09 (4.67)

[a] Be1 atom is coordinated with Ng atom
[b] B2 atom is coordinated with Ng atom
[c] B7 atom is coordinated with Ng atom
[d] B12 atom is coordinated with Ng atom

Table S4. Optimized Ng−Be Bond Length (R(Ng−Be), in Å), Binding Energy (BE, in kcal mol^{-1}), NPA charges on the Be atom and Ng Atom (q_{Be}, and q_{Ng}, in e) of Ng−Dianion1 (Ng−Be) Compounds using PBE0−D3/def−TZVPP (in C_{5v} Symmetry) and MP2/def−TZVPP (in C_5 Symmetry) Methods. MP2 Results are provided in the Parenthesis. ZPE Corrected BE are Reported with PBE0−D3/def−TZVPP Method

Ng−Dianion[a]	**R(Ng−Be)**	**BE**	**q_{Be}**	**q_{Be}**	**q_{Ng}**
			Dianion1	**Ng−Dianion1**	
He−Dianion1	1.552 (1.580)	−3.3 (−3.1)	1.69 (1.78)	1.73 (1.74)	0.08 (0.07)
Ne−Dianion1	1.900 (1.960)	−3.7 (−3.4)	1.69 (1.78)	1.76 (1.76)	0.05 (0.05)
Ar−Dianion1	2.116 (2.127)	−9.1 (−11.0)	1.69 (1.78)	1.69 (1.69)	0.13 (0.13)
Kr−Dianion1	2.238 (2.256)	−12.0 (−13.3)	1.69 (1.78)	1.65 (1.65)	0.17 (0.17)
Xe−Dianion1	2.407 (2.400)	−14.3 (−18.2)	1.69 (1.78)	1.61 (1.63)	0.22 (0.20)

[a] Be1 atom is coordinated with Ng atom

Table S5. Optimized Ng−B Bond Length (R(Ng−B), in Å), ZPE Corrected Binding Energy (BE, in kcal mol^{-1}), NPA charges on the B and Ng Atom (q_B and q_{Ng}, in e) of Ng−Dianion2[a] and Ng-Dianion3[b] Compounds Calculated using B3LYP−D3/def−TZVPP and PBE0/def−TZVPP Methods.

Ng−Dianion	**Method**	**R(Ng−B)**	**BE**	q_B	q_B	q_{Ng}
				Dianion	**Ng−Dianion**	
Ng−Dianion2						
He−Dianion2	B3LYP−D3	2.567	−0.1	0.46	0.56	0.03
	PBE0−D3	2.555	−0.8	0.47	0.57	0.03
Ne−Dianion2	B3LYP−D3	2.621	−1.2	0.46	0.52	0.03
	PBE0−D3	2.496	−1.5	0.47	0.52	0.04
Ar−Dianion2	B3LYP−D3	2.272	−4.8	0.46	0.29	0.25
	PBE0−D3	2.118	−6.8	0.47	0.11	0.33
Kr−Dianion2	B3LYP−D3	2.298	−8.2	0.46	0.17	0.37
	PBE0−D3	2.193	−11.1	0.47	0.05	0.44
Xe−Dianion2	B3LYP−D3	2.415	−12.3	0.46	0.07	0.50
	PBE0−D3	2.320	−16.1	0.47	−0.05	0.57
Ng−Dianion3						
He−Dianion3	B3LYP−D3	2.635	−0.3	0.75	0.86	0.03
	PBE0−D3	2.633	−1.1	0.77	0.88	0.03
Ne−Dianion3	B3LYP−D3	2.517	−1.4	0.75	0.82	0.04
	PBE0−D3	2.391	−1.8	0.77	0.82	0.05
Ar−Dianion3	B3LYP−D3	2.162	−6.6	0.75	0.51	0.32
	PBE0−D3	2.060	−9.2	0.77	0.41	0.38
Kr−Dianion3	B3LYP−D3	2.237	−10.5	0.75	0.41	0.43
	PBE0−D3	2.151	−13.8	0.77	0.31	0.49
Xe−Dianion3	B3LYP−D3	2.371	−15.0	0.75	0.33	0.55
	PBE0−D3	2.293	−20.7	0.77	0.23	0.61

[a] B2 atom is coordinated with Ng atom

[a] B7 atom is coordinated with Ng atom

Table S6. Optimized Ng−B Bond Length (R(Ng−B), in Å), Binding Energy (BE, in kcal mol^{-1}), NPA charges on the B and Ng Atom (q_B and q_{Ng}, in e) of Ng−Dianion4[a] Compounds using B3LYP−D3/def−TZVPP and PBE0/def−TZVPP, MP2/def−TZVPP Methods. ZPE Corrected BE are Reported with B3LYP−D3/def−TZVPP and PBE0/def−TZVPP Methods

Ng−Dianion4	Method	R(Ng−B)	BE	q_B	q_B	q_{Ng}
				Dianion4	Ng−Dianion4	
He−Dianion4	B3LYP−D3	2.248	−0.4	0.78	0.87	0.06
	PBE0−D3	1.666	−0.3	0.80	0.60	0.18
	MP2	2.434	−0.7	0.82	0.92	0.04
Ne−Dianion4	B3LYP−D3	2.371	−1.8	0.78	0.83	0.06
	PBE0−D3	2.249	−2.0	0.80	0.82	0.07
	MP2	2.329	−2.2	0.82	0.85	0.06
Ar−Dianion4	B3LYP−D3	2.118	−8.3	0.78	0.45	0.34
	PBE0−D3	2.026	−10.9	0.80	0.35	0.40
	MP2	1.986	−15.4	0.82	0.33	0.44
Kr−Dianion4	B3LYP−D3	2.206	−12.4	0.78	0.36	0.45
	PBE0−D3	2.132	−15.8	0.80	0.28	0.51
	MP2	2.087	−21.2	0.82	0.23	0.56
Xe−Dianion4	B3LYP−D3	2.347	−17.4	0.78	0.28	0.57
	PBE0−D3	2.275	−21.5	0.80	0.19	0.63
	MP2	2.209	−32.9	0.82	0.11	0.70

[a] B12 atom is coordinated with Ng atom

Table S7. Optimized Ng−B Bond Length (R(Ng−B), in Å), Binding Energy (BE, in kcal mol^{-1}), NPA charges on the B and Ng Atom (q_B and q_{Ng}, in e) of $[NgB_{12}(CN)_{11}]^-$ Compounds in C_{5v} Symmetry using B3LYP−D3/def−TZVPP and PBE0/def−TZVPP Methods and in C_5 symmetry using MP2 Method. PBE0−D3 Results are provided in the Parenthesis. ZPE Corrected Binding Energy are Reported with B3LYP−D3 and PBE0−D3 Methods.

$[NgB_{12}(CN)_{11}]^-$	Method	R(Ng−B)	BE	q_B	q_B	q_{Ng}
				$[B_{12}(CN)_{11}]^-$	$[NgB_{12}(CN)_{11}]^-$	
$[HeB_{12}(CN)_{11}]^-$	B3LYP−D3	1.623	−0.6	0.82	0.58	0.20
	(PBE0−D3)	(1.479)	(−1.7)	(0.84)	(0.46)	(0.26)
	MP2	1.555	−1.20	0.93	0.57	0.21
$[NeB_{12}(CN)_{11}]^-$	B3LYP−D3	2.085	−2.7	0.82	0.79	0.10
	(PBE0−D3)	(1.988)	(−3.2)	(0.84)	(0.76)	(0.12)
	MP2	2.075	−3.28	0.93	0.82	0.11
$[ArB_{12}(CN)_{11}]^-$	B3LYP−D3	2.048	−13.3	0.82	0.39	0.41
	(PBE0−D3)	(1.980)	(−16.4)	(0.84)	(0.32)	(0.46)
	MP2	1.948	−20.9	0.93	0.30	0.49
$[KrB_{12}(CN)_{11}]^-$	B3LYP−D3	2.153	−18.7	0.82	0.31	0.52
	(PBE0−D3)	(2.095)	(−22.4)	(0.84)	(0.24)	(0.57)
	MP2	2.061	−27.8	0.93	0.20	0.61
$[XeB_{12}(CN)_{11}]^-$	B3LYP−D3	2.313	−25.2	0.82	0.24	0.66
	(PBE0−D3)	(2.249)	(−29.5)	(0.84)	(0.16)	(0.70)
	MP2	2.194	−40.8	0.93	0.10	0.76

Table S8. Optimized Ng−B Bond Length (R(Ng−B), in Å), Binding Energy (BE, in kcal mol^{-1}), NPA charges on the B and Ng Atom (q_{B} and q_{Ng}, in e) of $[NgB_{12}(Cl)_{11}]^{-}$ Compounds in C_{5v} Symmetry using B3LYP−D3/def−TZVPP and PBE0/def−TZVPP Methods and in C_{5} symmetry using MP2 Method. PBE0−D3 Results are provided in the Parenthesis. ZPE Corrected Binding Energy are Reported with B3LYP−D3 and PBE0−D3 Methods.

$[NgB_{12}(Cl)_{11}]^{-}$	Method	R(Ng−B)	BE	q_{B}	q_{B}	q_{Ng}
				$[B_{12}(Cl)_{11}]^{-}$	$[NgB_{12}(Cl)_{11}]^{-}$	
$[HeB_{12}(Cl)_{11}]^{-}$	B3LYP−D3	2.163	−0.4	0.67	0.76	0.07
	(PBE0−D3)	(1.564)	(−0.2)	(0.70)	(0.41)	(0.21)
	MP2	2.323	−0.6	0.72	0.84	0.05
$[NeB_{12}(Cl)_{11}]^{-}$	B3LYP−D3	2.317	−1.7	0.67	0.72	0.06
	(PBE0−D3)	(2.227)	(−1.8)	(0.70)	(0.71)	(0.07)
	MP2	2.280	−2.1	0.72	0.75	0.07
$[ArB_{12}(Cl)_{11}]^{-}$	B3LYP−D3	2.095	−8.4	0.67	0.30	0.35
	(PBE0−D3)	(2.015)	(−10.7)	(0.70)	(0.21)	(0.40)
	MP2	1.969	−15.6	0.72	0.22	0.40
$[KrB_{12}(Cl)_{11}]^{-}$	B3LYP−D3	2.189	−12.5	0.67	0.21	0.45
	(PBE0−D3)	(2.116)	(−15.5)	(0.70)	(0.12)	(0.50)
	MP2	2.073	−21.4	0.72	0.05	0.55
$[XeB_{12}(Cl)_{11}]^{-}$	B3LYP−D3	2.333	−17.3	0.67	0.14	0.56
	(PBE0−D3)	(2.263)	(−21.1)	(0.70)	(0.05)	(0.62)
	MP2	2.196	−32.4	0.72	0.01	0.64

Table S9. Optimized Ng−B Bond Length (R(Ng−Be), in Å), ZPE Corrected Binding Energy (BE, in kcal mol^{-1}), NPA charges on the Be, Li and Ng Atoms (q_B, q_{Li} and q_{Ng}, in e) of {Li^+@$[NgBeB_{11}(CN)_{11}]^{2-}$} Compounds using B3LYP−D3/def−TZVPP and Method.

Systems	R(Ng−Be)	q_{Be}	q_{Li}	q_{Ng}	BE
{Li^+@$[BeB_{11}(CN)_{11}]^{2-}$}	**...**	1.79	0.91	**...**	**...**
{Li^+@$[HeBeB_{11}(CN)_{11}]^{2-}$}	1.538	1.73	0.91	0.08	−3.4
{Li^+@$[NeBeB_{11}(CN)_{11}]^{2-}$}	1.889	1.76	0.91	0.05	−4.1
{Li^+@$[ArBeB_{11}(CN)_{11}]^{2-}$}	2.111	1.68	0.91	0.13	−10.6
{Li^+@$[KrBeB_{11}(CN)_{11}]^{2-}$}	2.244	1.65	0.91	0.17	−13.1
{Li^+@$[XeBeB_{11}(CN)_{11}]^{2-}$}	2.421	1.61	0.91	0.23	−15.7

Table S10. ZPE Corrected Relative Energy (RE, in kcal mol$^{-1)}$ of Ng_2−Anion3[a] $[1,12-(Ng)_2BeB_{11}(CN)_{10}]^-$ with respect to Ng_2−Anion2[b] $[1,7-(Ng)_2BeB_{11}(CN)_{10}]^-$ at B3LYP−D3/def−TZVPP level of theory. PBE0−D3/def−TZVPP Calculated Values are Provided Within Parenthesis. HOMO-LUMO Energy Gap (ΔE_{gap}, in eV) using B3LYP-D3/def-TZVPP (PBE0-D3/def-TZVPP) Level of Theory is also Reported.

Ng−Dianion		**$[1,7-(Ng)_2BeB_{11}(CN)_{10}]^-$**	**$[1,12-(Ng)_2BeB_{11}(CN)_{10}]^-$**
		Ng_2−Anion2	**Ng_2−Anion3**
Anion	**RE**	0.0 (0.0)	2.5 (2.8)
	ΔE_{gap}	3.26 (3.63)	3.17 (3.53)
He_2−Anion	**RE**	0.00 (0.0)	2.11 (2.1)
	ΔE_{gap}	3.95 (4.94)	4.50 (5.47)
Ne_2−Anion	**RE**	0.0 (0.0)	2.09 (2.2)
	ΔE_{gap}	3.74 (4.23)	3.81 (4.35)
Ar_2−Anion	**RE**	0.0 (0.0)	0.8 (0.7)
	ΔE_{gap}	4.84 (5.44)	4.92 (5.55)
Kr_2−Anion	**RE**	0.0 (0.0)	0.6 (0.5)
	ΔE_{gap}	4.85 (5.41)	4.91 (5.49)
Xe_2−Anion	**RE**	0.0 (0.0)	0.4 (0.3)
	ΔE_{gap}	4.70 (5.24)	4.76 (5.29)

[a] Be1 and B12 atoms are coordinated with Ng atom

[b] Be1 and B7 atoms are coordinated with Ng atom

Table S11. Optimized Ng−B, Ng−Be Bond Length (R(Ng−B) and R(Ng−Be), in Å), ZPE Corrected Binding Energy (BE, in kcal mol^{-1}), NPA charges on the B, Be and Ng Atoms (q_{B}, q_{Be} and q_{Ng}, in e) of $[1,7\text{-}(Ng)_2BeB_{11}(CN)_{10}]^{-a}$ Compounds using B3LYP−D3/def−TZVPP and PBE0−D3/def−TZVPP Methods

Method	R(Ng−Be)	R(Ng−B)	BE	q_{Be}	q_{B}	$q_{Ng(Be)}$[b]	$q_{Ng(B)}$[c]	q_{Be}	q_{B}
				$[BeB_{11}(CN)_{10}]^{-}$		$[(Ng)_2BeB_{11}(CN)_{10}]^{-}$			
$[(He)_2BeB_{11}(CN)_{10}]^{-}$									
B3LYP−D3	1.532	1.901	−4.4	1.79	0.80	0.08	0.12	1.73	0.76
PBE0−D3	1.530	1.611	−5.4	1.80	0.82	0.08	0.20	1.73	0.57
$[(Ne)_2BeB_{11}(CN)_{10}]^{-}$									
B3LYP−D3	1.875	2.212	−6.9	1.79	0.80	0.05	0.08	1.76	0.80
PBE0−D3	1.860	2.102	−7.3	1.80	0.82	0.05	0.10	1.76	0.78
$[(Ar)_2BeB_{11}(CN)_{10}]^{-}$									
B3LYP−D3	2.109	2.087	−22.3	1.79	0.80	0.13	0.37	1.68	0.43
PBE0−D3	2.085	2.011	−25.8	1.80	0.82	0.14	0.43	1.68	0.35
$[(Kr)_2BeB_{11}(CN)_{10}]^{-}$									
B3LYP−D3	2.242	2.183	−29.7	1.79	0.80	0.17	0.48	1.65	0.35
PBE0−D3	2.215	2.118	−34.1	1.80	0.82	0.18	0.54	1.64	0.26
$[(Xe)_2BeB_{11}(CN)_{10}]^{-}$									
B3LYP−D3	2.420	2.331	−38.2	1.79	0.80	0.23	0.61	1.61	0.27
PBE0−D3	2.389	2.269	−43.6	1.80	0.82	0.24	0.66	1.59	0.19

[a] Be1 and B7 atoms are coordinated with Ng atom

[b] qNg(Be) represents charge on Ng atom which is connected with Be atom

[c] qNg(B) represents charge on Ng atom which is connected with B atom

The BE of $[1,7\text{-}(Ng)_2BeB_{11}(CN)_{10}]^{-}$ (Ng_2-Anion**2**) is calculated using the given Equation S2.

The ZPE corrected BE monotonically increases from $[He_2BeB_{11}(CN)_{10}]^{-}$ to $[Xe_2BeB_{11}(CN)_{10}]^{-}$ compounds. The Ng-B, Ng-Be bond length, NPA analysis and BE show high stability of $[(Ng)_2BeB_{11}(CN)_{10}]^{-}$ compounds than the corresponding dianionic $[NgBeB_{11}(CN)_{11}]^{2-}$ compounds.

Table S12. Optimized Ng−B, Ng−Be Bond Length (R(Ng−B) and R(Ng−Be), in Å), Binding Energy (BE, in kcal mol^{-1}), NPA charges on the B, Be and Ng Atoms (q_{B}, q_{Be} and q_{Ng}, in e) of $[1,12\text{-}(Ng)_2BeB_{11}(CN)_{10}]^{-}$[a] Compounds in C_{5v} Symmetry using B3LYP−D3/def−TZVPP, PBE0−D3/def−TZVPP Methods and in C_5 symmetry using MP2 Method. ZPE Corrected Binding Energy are Reported with B3LYP−D3 and PBE0−D3 Methods.

Method	R(Ng−Be)	R(Ng−B)	BE	q_{Be}	q_{B}	$q_{Ng(Be)}$[b]	$q_{Ng(B)}$[c]	q_{Be1}	q_{B}
				$[BeB_{11}(CN)_{10}]^{-}$		$[(Ng)_2BeB_{11}(CN)_{10}]^{-}$			
$[(He)_2BeB_{11}(CN)_{10}]^{-}$									
B3LYP−D3	1.532	1.646	−4.7	1.80	0.82	0.08	0.19	1.73	0.59
PBE0−D3	1.531	1.478	−6.1	1.80	0.85	0.08	0.26	1.73	0.45
MP2	1.549	1.525	−5.8	1.80	0.86	0.07	0.22	1.74	0.53
$[(Ne)_2BeB_{11}(CN)_{10}]^{-}$									
B3LYP−D3	1.864	2.123	−7.3	1.80	0.82	0.05	0.09	1.76	0.79
PBE0−D3	1.851	2.002	−8.0	1.80	0.85	0.05	0.12	1.76	0.75
MP2	1.885	2.061	−7.8	1.80	0.86	0.06	0.11	1.76	0.81
$[(Ar)_2BeB_{11}(CN)_{10}]^{-}$									
B3LYP−D3	2.106	2.062	−24.0	1.80	0.82	0.14	0.39	1.68	0.39
PBE0−D3	2.084	1.992	−28.0	1.80	0.85	0.14	0.44	1.68	0.32
MP2	2.097	1.954	−34.3	1.80	0.86	0.14	0.48	1.68	0.29
$[(Kr)_2BeB_{11}(CN)_{10}]^{-}$									
B3LYP−D3	2.242	2.160	−31.6	1.80	0.82	0.17	0.50	1.65	0.30
PBE0−D3	2.215	2.103	−36.5	1.80	0.85	0.18	0.55	1.64	0.23
MP2	2.230	2.065	−43.7	1.80	0.86	0.18	0.60	1.65	0.20
$[(Xe)_2BeB_{11}(CN)_{10}]^{-}$									
B3LYP−D3	2.419	2.316	−40.3	1.80	0.82	0.23	0.63	1.61	0.24
PBE0−D3	2.387	2.261	−46.2	1.80	0.85	0.24	0.68	1.60	0.16
MP2	2.380	2.198	−61.8	1.80	0.86	0.24	0.75	1.60	0.09

[a] Be1 and B12 atoms are coordinated with Ng atom

[b] *q*Ng(Be) represents charge on Ng atom which is connected with Be atom

[c] *q*Ng(B) represents charge on Ng atom which is connected with B atom

The BE of $[1,12\text{-}(Ng)_2BeB_{11}(CN)_{10}]^{-}$ (Ng_2-Anion**3)** is calculated using the given Equation S2.

The ZPE corrected BE monotonically increases from $[He_2BeB_{11}(CN)_{10}]^{-}$ to $[Xe_2BeB_{11}(CN)_{10}]^{-}$ compounds. The Ng-B, Ng-Be bond length, NPA analysis and BE show high stability of $[(Ng)_2BeB_{11}(CN)_{10}]^{-}$ compounds than the corresponding dianionic $[NgBeB_{11}(CN)_{11}]^{2-}$ compounds.

Table S13. Calculated Values of Bond Critical Point Electron Density (ρ in e a_0^{-3}), Laplacian of Electron Density ($\nabla^2\rho$ in e a_0^{-5}), Local Electron Energy Density (E_d in au), and Ratio of Local Electron Kinetic Energy Density and Electron Density (G(r)/ρ in au) of Ng−B and Ng−Be bond in Ng−Dianion1, Ng−Dianion2, $[NgB_{12}(CN)_{11}]^-$, $[NgB_{12}(Cl)_{11}]^-$ and $[1,12\text{-}(Ng)_2BeB_{11}(CN)_{10}]^-$ (Ng$_2$-Anion3) using ^{a}B3LYP−D3/def−TZVPP method.

Ng−Compound	Bond	ρ	$\nabla^2\rho$	^{b}G(r)	^{c}V(r)	^{d}E$_d$(r)	G(r)/ρ	^{e}Type
He−Dianion1	**He−Be**	0.025	0.303	0.061	−0.047	0.014	2.440	**W^n**
Ne−Dianion1	**Ne−Be**	0.016	0.179	0.036	−0.028	0.008	2.250	**W^n**
Ar−Dianion1	**Ar−Be**	0.026	0.194	0.044	−0.040	0.004	1.692	**W^n**
Kr−Dianion1	**Kr−Be**	0.027	0.164	0.040	−0.039	0.001	1.481	**W^n**
Xe−Dianion1	**Xe−Be**	0.027	0.124	0.034	−0.036	−0.003	1.259	**W^c**
He−Dianion2	**He−B**	0.011	0.038	0.008	−0.007	0.001	0.727	**D**
Ne−Dianion2	**Ne−B**	0.013	0.046	0.011	−0.010	0.001	0.846	**D**
Ar−Dianion2	**Ar−B**	0.049	0.076	0.047	−0.076	−0.028	0.959	**C**
Kr−Dianion2	**Kr−B**	0.056	0.026	0.042	−0.078	−0.036	0.750	**C**
Xe−Dianion2	**Xe−B**	0.062	−0.034	0.027	−0.063	−0.036	0.435	**C**
$[HeB_{12}(CN)_{11}]^-$	**He−B**	0.036	0.160	0.054	−0.067	−0.014	1.500	**W^c**
$[NeB_{12}(CN)_{11}]^-$	**Ne−B**	0.024	0.066	0.020	−0.024	−0.004	0.833	**D**
$[ArB_{12}(CN)_{11}]^-$	**Ar−B**	0.058	0.112	0.065	−0.102	−0.037	1.121	**W^c**
$[KrB_{12}(CN)_{11}]^-$	**Kr−B**	0.065	0.258	0.052	−0.098	−0.046	0.800	**C**
$[XeB_{12}(CN)_{11}]^-$	**Xe−B**	0.070	−0.059	0.029	−0.072	−0.044	0.414	**C**
$[HeB_{12}Cl_{11}]^-$	**He−B**	0.013	0.043	0.010	−0.009	0.001	0.769	**D**
$[NeB_{12}Cl_{11}]^-$	**Ne−B**	0.015	0.049	0.012	−0.012	0.000	0.800	**D**
$[ArB_{12}Cl_{11}]^-$	**Ar−B**	0.051	0.092	0.053	−0.083	−0.030	1.039	**W^c**
$[KrB_{12}Cl_{11}]^-$	**Kr−B**	0.058	0.034	0.046	−0.083	−0.037	0.793	**C**
$[XeB_{12}Cl_{11}]^-$	**Xe−B**	0.063	−0.033	0.029	−0.066	−0.037	0.460	**C**
He$_2$-Anion3	**He−Be**	0.028	0.330	0.067	−0.052	0.015	2.393	**W^n**
	He−B	0.035	0.141	0.048	−0.061	−0.012	1.371	**W^c**

Ne_2-Anion3	**Ne−Be**	0.019	0.218	0.044	−0.033	0.010	2.316	**W**^{n}
	Ne−B	0.022	0.063	0.019	−0.021	−0.003	0.864	**D**
Ar_2-Anion3	**Ar−Be**	0.029	0.213	0.049	−0.045	0.004	1.690	**W**^{n}
	Ar−B	0.056	0.109	0.062	−0.097	−0.035	1.107	**W**^{c}
Kr_2-Anion3	**Kr−Be**	0.030	0.172	0.043	−0.043	0.000	1.433	**W**^{n}
	Kr−B	0.063	0.032	0.052	−0.096	−0.044	0.825	**C**
Xe_2-Anion3	**Xe−Be**	0.030	0.126	0.036	−0.040	−0.004	1.200	**W**^{c}
	Xe−B	0.068	−0.051	0.029	−0.071	−0.042	0.426	**C**

[a] For Xe atom def2−TZVPP basis is used along with 60−electron core ECP.

[b] G(**r**) represents the local electron kinetic energy density.

[c] V(**r**) signifies the local electron potential energy density.

[d] "Type" is an indication of type of weak covalent bonding exists in between the corresponding pair of bonding atoms.

If $E_d(r) < 0$ and $G(r)/\rho(r) < 1$ then the bond is termed as "C type" covalent bond, while if $|E_d(r)| < 0.005$ and $G(r)/\rho(r) < 1$, then the bond is "D type" covalent bond even if $\nabla^2\rho(r) > 0$.[9b] In addition to this, Boggs et al[9b] proposed that if $E_d(r) > 0$ and $G(r)/\rho(r) > 1$, then the bond is a weak interaction with some noncovalent character represented as "W^n type", whereas if $E_d(r) < 0$ and $G(r)/\rho(r) > 1$, then it is weak interaction with some covalent character represented as "W^c type".

Table S14. The Calculated Values of Electrostatic Energy (ΔE^{elec}), Pauli Repulsion Energy (ΔE^{Pauli}), Orbital Interactions Energy (ΔE^{orb}), Dispersion Energy (ΔE^{disp}) and Total Interaction Energy (ΔE^{int}) of Ng−Dianion2[a] Compounds in kcal mol^{-1} as obtained from Energy Decomposition Analysis at B3LYP−D3/def−TZVPP level of theory. (Percentage Contribution of ΔE^{elec}, ΔE^{orb} and ΔE^{disp} Energy term to the Total Interaction Energy are Provided within Parenthesis)

Ng−Dianion2	**ΔE^{Pauli}**	**ΔE^{elstat}**	**ΔE^{orb}**	**ΔE^{disp}**	**ΔE^{int}**
He−Dianion2	1.2	−0.3 (18.6)	−0.6 (36.6)	−0.8 (44.8)	−0.6
Ne−Dianion2	2.2	−1.0 (29.7)	−1.0 (28.2)	−1.4 (42.1)	−1.1
Ar−Dianion2	29.8	−11.5 (31.5)	−20.0 (54.8)	−5.0 (13.8)	−6.7
Kr−Dianion2	43.7	−17.0 (30.7)	−31.7 (57.1)	−6.8 (12.2)	−11.7
Xe−Dianion2	53.9	−21.1 (29.5)	−42.3 (59.0)	−8.3 (11.5)	−17.8

[a] B2 atom is coordinated with Ng atom

Here, $\Delta E^{int} = \Delta E^{Pauli} + \Delta E^{elstat} + \Delta E^{orb} + \Delta E^{disp}$

$\Delta E^{orb} = \Delta E^{\sigma} + \Delta E^{\pi}$

In case of He and Ne-Dianion**2**, maximum contribution of ΔE^{disp} toward ΔE^{int}, shows very weak nature of He-B and Ne-B interaction. However, as we move from He-Xe, the contribution of ΔE^{orb} toward ΔE^{int} increases, while contribution of ΔE^{disp} decreases, which indicates increase in the covalency of Ng-B bond along the same.

Table S15. The Calculated Values of Electrostatic Energy (ΔE^{elec}), Pauli Repulsion Energy (ΔE^{Pauli}), Orbital Interactions Energy (ΔE^{orb}), Dispersion Energy (ΔE^{disp}) and Total Interaction Energy (ΔE^{int}) of $[1,7\text{-}(Ng)_2BeB_{11}(CN)_{10}]^-$ [a] (Ng_2−Anion2) Compounds in kcal mol^{-1} as obtained from Energy Decomposition Analysis at B3LYP−D3/def−TZVPP level of theory. (Percentage Contribution of ΔE^{elec}, ΔE^{orb} and ΔE^{disp} Energy term to the Total Interaction Energy are Provided within Parenthesis)

Ng_2−Anion2	**ΔE^{Pauli}**	**ΔE^{elstat}**	**ΔE^{orb}**	**ΔE^{disp}**	**ΔE^{int}**
He_2−Anion2	17.0	−3.8 (16.1)	−17.3 (74.5)	−2.2 (9.4)	−6.3
Ne_2−Anion2	15.1	−5.2 (23.2)	−13.6 (61.3)	−3.4 (15.4)	−7.4
Ar_2−Anion2	61.7	−19.5 (22.2)	−59.0 (67.0)	−9.5 (10.8)	−26.0
Kr_2−Anion2	72.6	−22.9 (21.2)	−72.7 (67.3)	−12.4 (11.5)	−35.4
Xe_2−Anion2	81.5	−25.5 (19.9)	−87.3 (68.3)	−15.1 (11.8)	−46.4

[a] Be1 and B7 atoms are coordinated with Ng atom

Here, $\Delta E^{int} = \Delta E^{Pauli} + \Delta E^{elstat} + \Delta E^{orb} + \Delta E^{disp}$

$\Delta E^{orb} = \Delta E^{\sigma} + \Delta E^{\pi}$

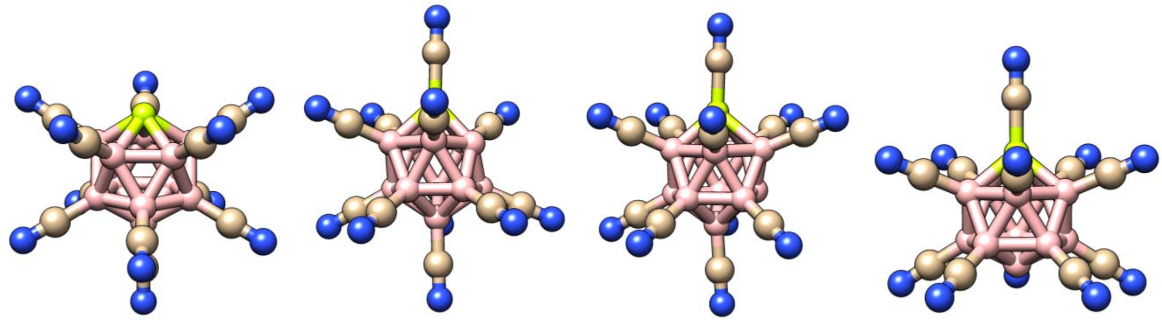

RE	**0.0 (0.0)**	**25.6 (30.1)**	**33.9 (38.4)**	**39.3 (43.9)**
Isomer	**Dianion1**	**Dianion2**	**Dianion3**	**Dianion4**

Figure S1. Optimized Structures of Dianion**1** (with free Be1 atom), Dianion**2** (with free B2 atom), Dianion**3** (with free B7 atom) and Dianion**4** (with free B12 atom) of $[BeB_{11}(CN)_{11}]^{2-}$ at B3LYP-D3/def-TZVPP level of theory. Relative energy (RE, in kcal mol^{-1}) calculated using B3LYP-D3/def-TZVPP (PBE0-D3/def-TZVPP) is also reported.

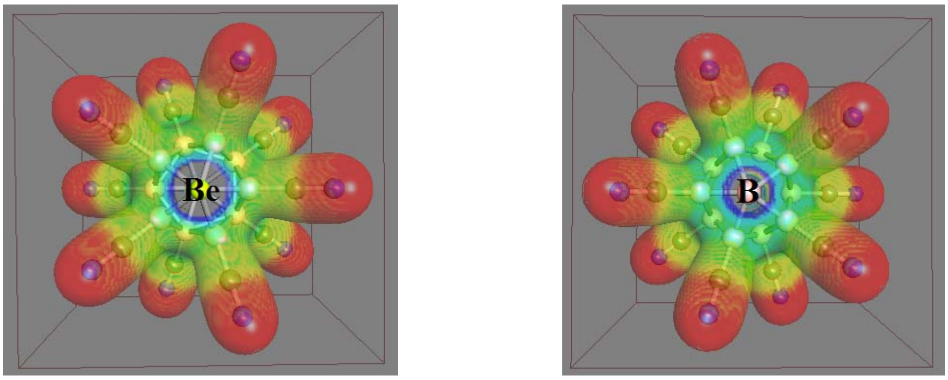

Figure S2. ESP of Dianion**1** (on left) and Dianion**4** (on right) of $[BeB_{11}(CN)_{11}]^{2-}$. Red region is a electron−rich nucleophilic site and blue region is electron−deficient electrophilic site

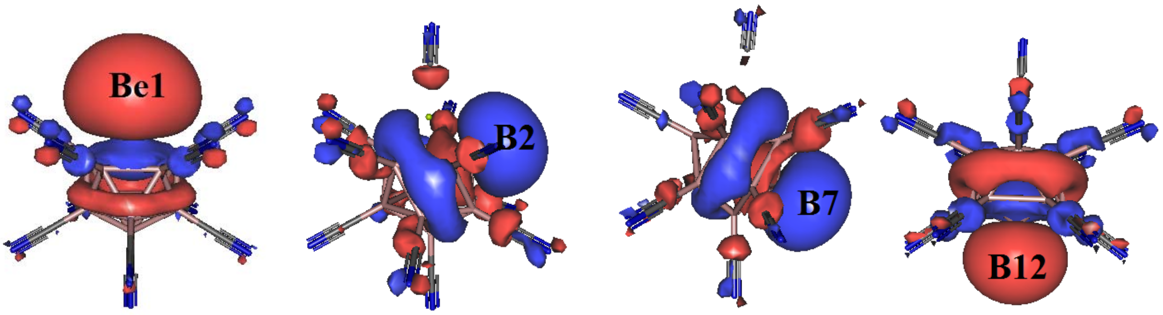

Dianion1 **Dianion2** **Dianion3** **Dianion4**

Figure S3. Pictures of lowest unoccupied molecular orbital (LUMO) of different Isomers of Dianion $[BeB_{11}(CN)_{11}]^{2-}$ at B3LYP-D3/def-TZVPP level of theory.

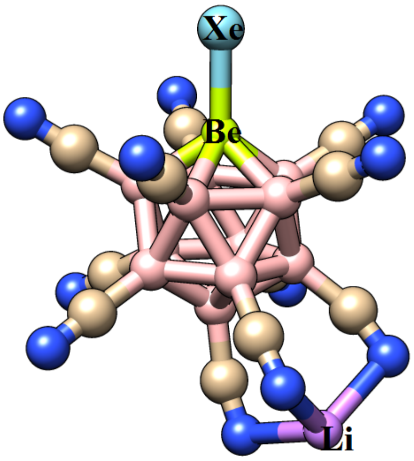

Figure S4. Optimized structures of $\{Li^{+}[XeBeB_{11}(CN)_{11}]^{2-}\}$ at B3LYP-D3/def-TZVPP level of theory.

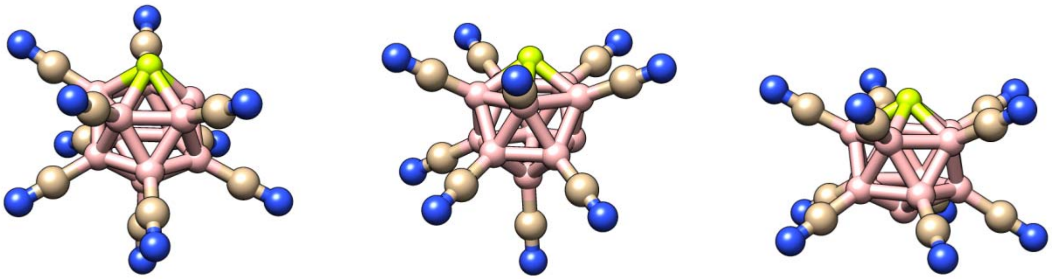

RE **0.5 (0.4)** **0.0 (0.0)** **2.5 (2.8)**

Anion1 **Anion2** **Anion3**

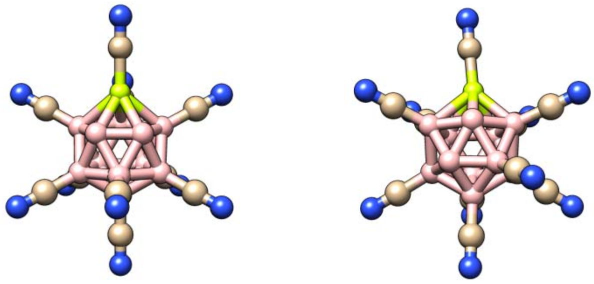

RE **31.7 (36.5)** **37.4 (42.5)**

Anion4 **Anion5**

Figure S5. Optimized Structures of Anion**1** [1,2-$BeB_{11}(CN)_{10}$]$^{-}$, Anion**2** [1,7-$BeB_{11}(CN)_{10}$]$^{-}$, Anion**3** [1,12-$BeB_{11}(CN)_{10}$]$^{-}$, and Anion**4** [5,6-$BeB_{11}(CN)_{10}$]$^{-}$, Anion**5** [5,10-$BeB_{11}(CN)_{10}$]$^{-}$ at B3LYP-D3/def-TZVPP level of theory. Relative energy (RE, in kcal mol^{-1}) calculated using B3LYP-D3/def-TZVPP (PBE0-D3/def-TZVPP) is also reported.

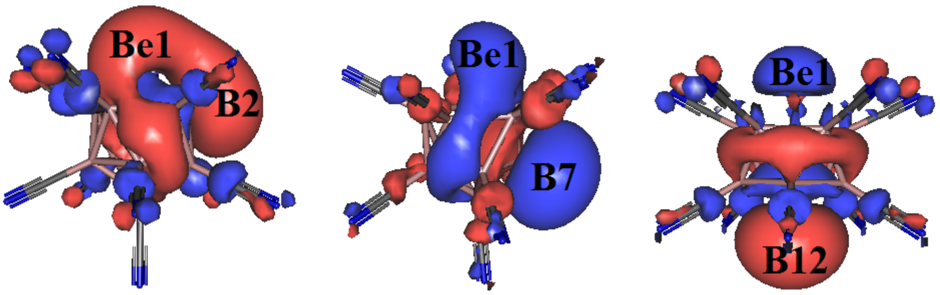

Anion1 **Anion2** **Anion3**

Figure S6. Pictures of lowest unoccupied molecular orbital (LUMO) of different Isomers of Anion [$BeB_{11}(CN)_{10}$]$^{-}$ at B3LYP-D3/def-TZVPP level of theory.

.

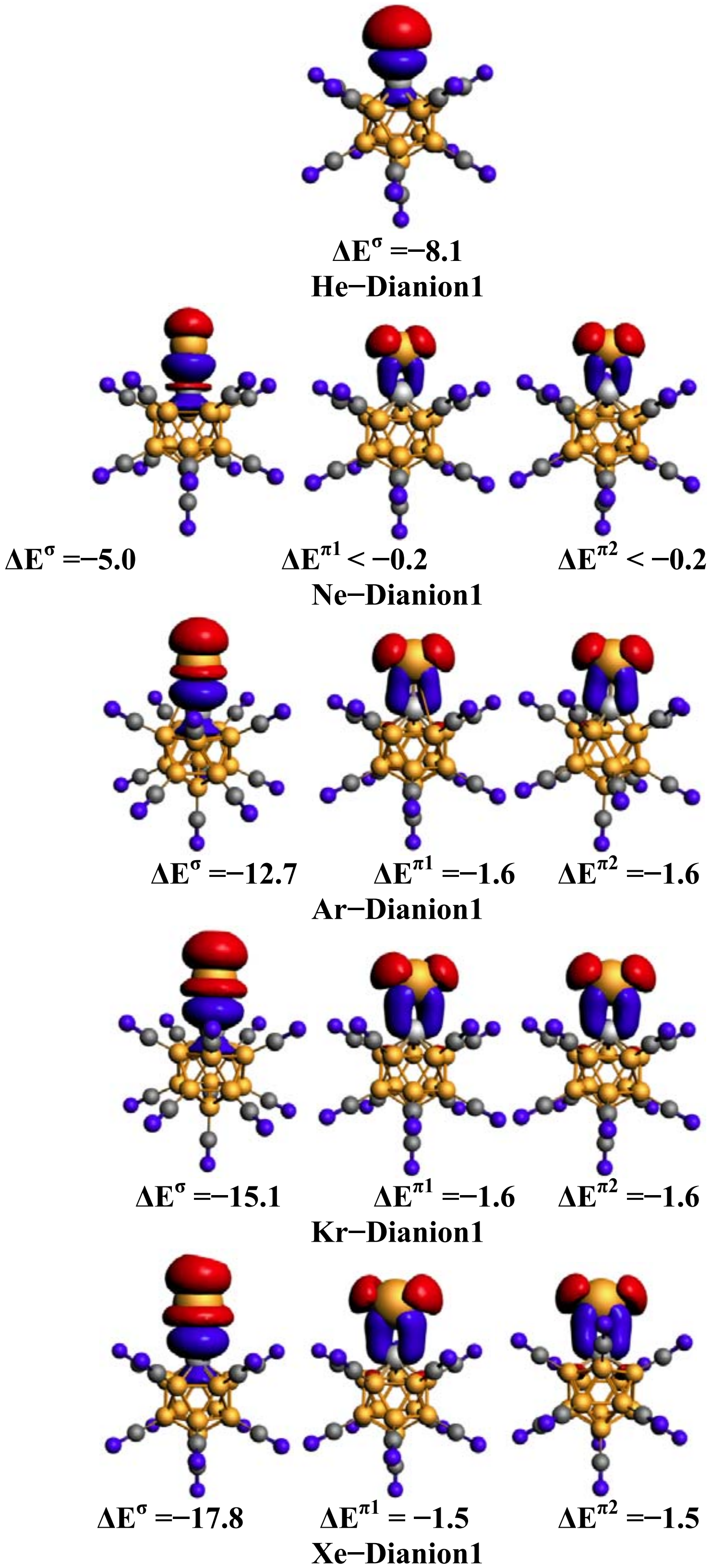

Figure S7. Deformation densities ($\Delta\rho(r)$) plots of the pairwise orbital interactions for Ng−Dianion**1** (Ng =He−Xe) complexes and the associated ΔE^{orb} energies (ΔE^{σ} and ΔE^{π}, in kcal mol^{-1}) obtained from the EDA−NOCV at B3LYP-D3/TZ2P level of theory. The blue and red colored surfaces indicate regions with $\Delta\rho(r) > 0$ and $\Delta\rho(r) < 0$, respectively.

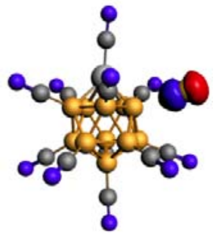

$\Delta E^{\sigma} < -0.2$

He−Dianion2

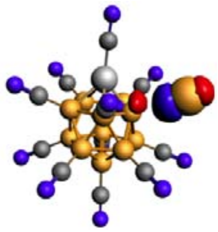

$\Delta E^{\sigma} = -0.7$

Ne−Dianion2

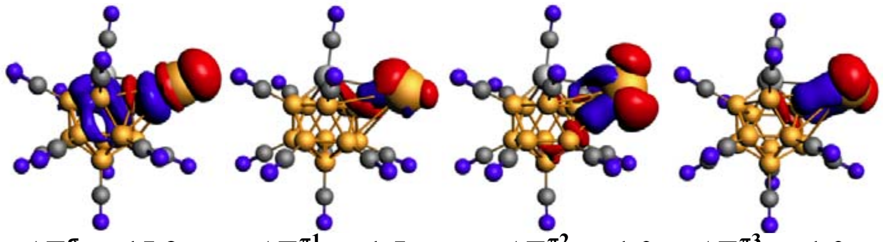

$\Delta E^{\sigma} = -15.9$ **$\Delta E^{\pi1} = -1.5$** **$\Delta E^{\pi2} = -1.0$** **$\Delta E^{\pi3} = -1.0$**

Ar−Dianion2

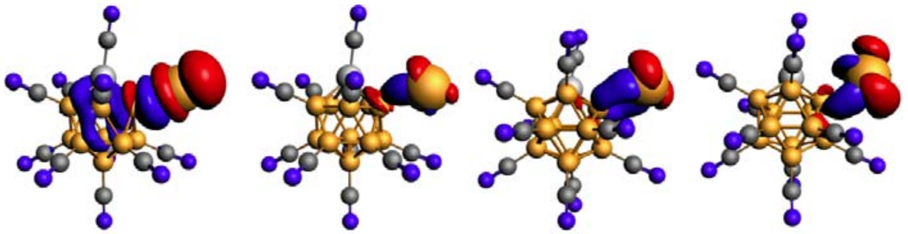

$\Delta E^{\sigma} = -25.7$ **$\Delta E^{\pi1} = -2.1$** **$\Delta E^{\pi2} = -1.6$** **$\Delta E^{\pi3} = -1.4$**

Kr−Dianion2

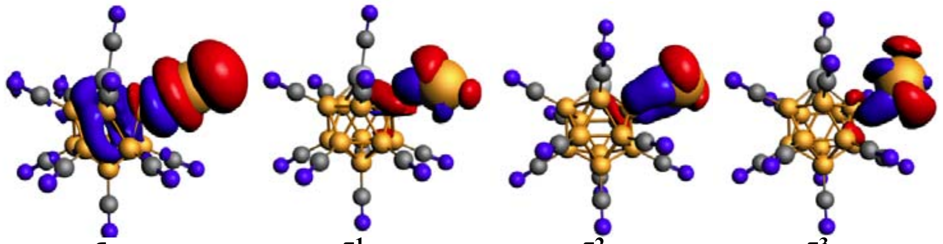

$\Delta E^{\sigma} = -35.3$ **$\Delta E^{\pi1} = -2.5$** **$\Delta E^{\pi2} = -1.9$** **$\Delta E^{\pi3} = -1.6$**

Xe−Dianion2

Figure S8. Deformation densities ($\Delta\rho(r)$) plots of the pairwise orbital interactions for Ng−Dianion**2** (Ng =He−Xe) complexes and the associated ΔE^{orb} energies (ΔE^{σ} and ΔE^{π}, in kcal mol^{-1}) obtained from the EDA−NOCV at B3LYP-D3/TZ2P level of theory. The blue and red colored surfaces indicate regions with $\Delta\rho(r) > 0$ and $\Delta\rho(r) < 0$, respectively.

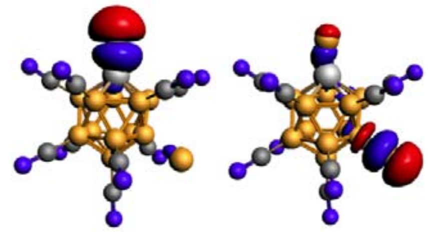

$\Delta E^{\sigma 1} = -9.4$ $\Delta E^{\sigma 2} = -5.5$

He$_2$−Anion2

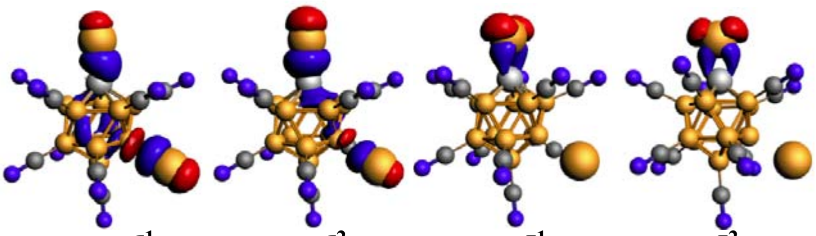

$\Delta E^{\sigma 1} = -4.7$ $\Delta E^{\sigma 2} = -5.6$ $\Delta E^{\pi 1} < 0.1$ $\Delta E^{\pi 2} < 0.1$

Ne$_2$−Anion2

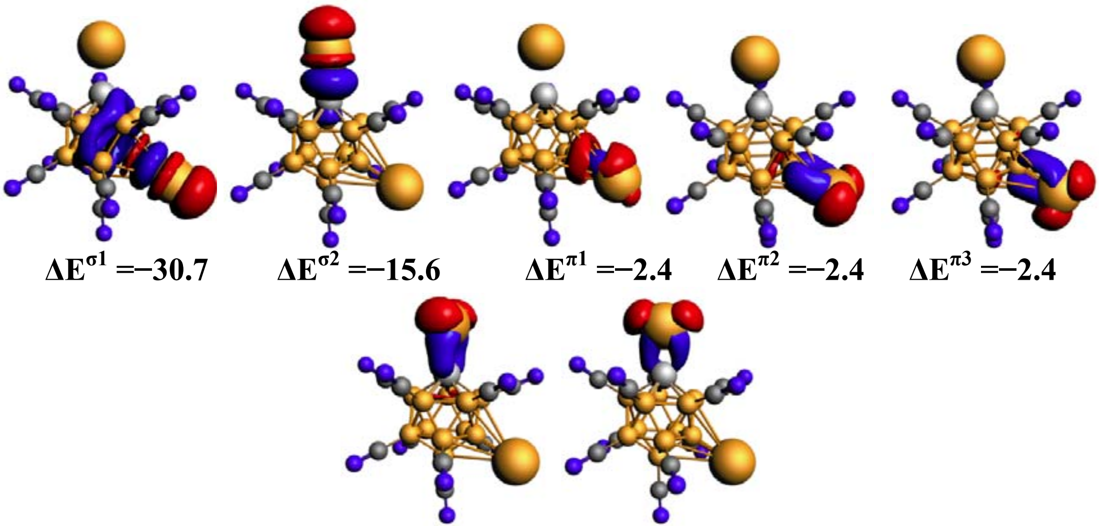

$\Delta E^{\sigma 1} = -30.7$ $\Delta E^{\sigma 2} = -15.6$ $\Delta E^{\pi 1} = -2.4$ $\Delta E^{\pi 2} = -2.4$ $\Delta E^{\pi 3} = -2.4$

$\Delta E^{\pi 4} = -2.1$ $\Delta E^{\pi 5} = -1.9$

Ar$_2$−Anion2

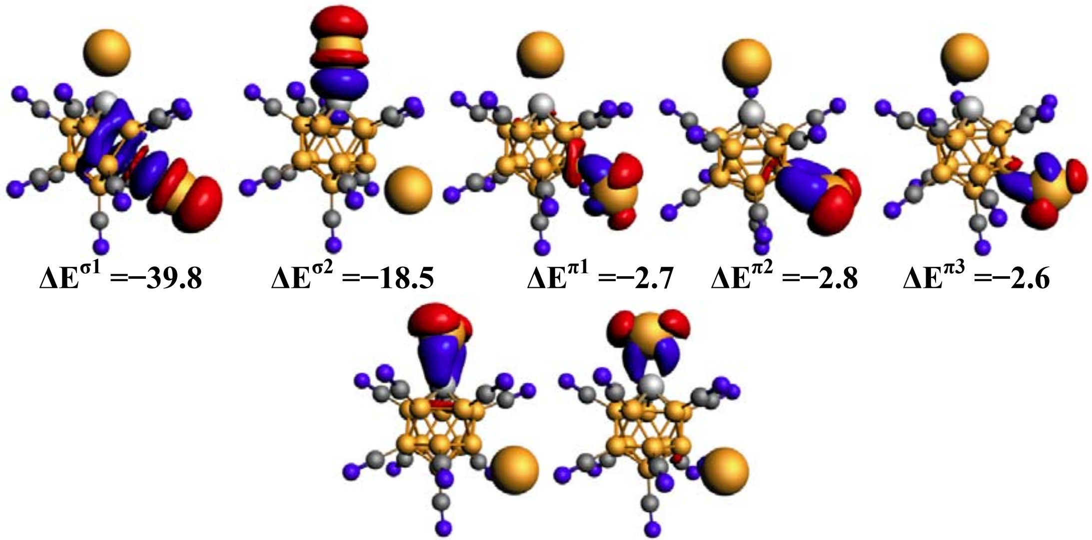

$\Delta E^{\sigma 1} = -39.8$ $\Delta E^{\sigma 2} = -18.5$ $\Delta E^{\pi 1} = -2.7$ $\Delta E^{\pi 2} = -2.8$ $\Delta E^{\pi 3} = -2.6$

$\Delta E^{\pi 4} = -2.3$ $\Delta E^{\pi 5} = -2.0$

Kr$_2$−Anion2

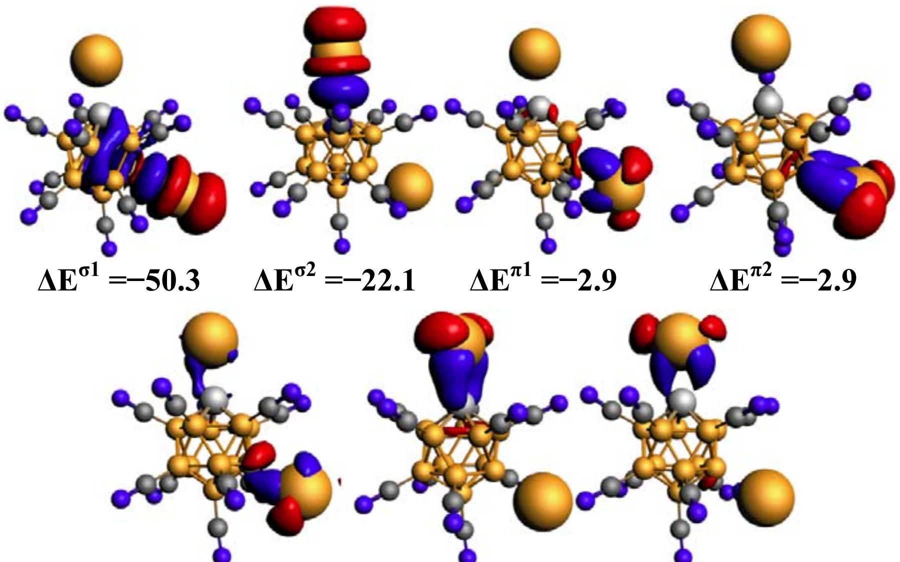

$\Delta E^{\sigma 1} = -50.3$ **$\Delta E^{\sigma 2} = -22.1$** **$\Delta E^{\pi 1} = -2.9$** **$\Delta E^{\pi 2} = -2.9$**

$\Delta E^{\pi 3} = -2.5$ **$\Delta E^{\pi 4} = -2.2$** **$\Delta E^{\pi 5} = -1.9$**

Xe_2−Anion2

Figure S9. Deformation densities ($\Delta\rho$(r)) plots of the pairwise orbital interactions for Ng_2−Anion**2** (Ng =He−Xe) complexes and the associated ΔE^{orb} energies (ΔE^{σ} and ΔE^{π}, in kcal mol^{-1}) obtained from the EDA−NOCV at B3LYP-D3/TZ2P level of theory. The blue and red colored surfaces indicate regions with $\Delta\rho$(r) > 0 and $\Delta\rho$(r) < 0, respectively.